Journal of Radioanalytical and Nuclear Chemistry, Articles, Vol. 185, No. 2 (1994) 273–291

PARTICLE-INDUCED-GAMMA-RAY-EMISSION SPECTROMETRY APPLIED TO THE DETERMINATION OF LIGHT ELEMENTS IN INDIVIDUAL GRAINS OF GRANITE MINERALS

M. VOLFINGER, J.-L. ROBERT

CRSCM–CNRS, 1A rue de la Férollerie, 45071 Orléans cedex 2 (France)

(Received July 18, 1994)

The quantitative determination of Li, Be, B, F is feasible using a sensitive and non-destructive method by the analysis of the prompt γ-rays induced with charged particles (PIGE). The irradiation source is a Van de Graaff accelerator, and γ-analysis has to be performed during the irradiation. Measurements were made at the CERI laboratory in Orléans with the PIGE method using a $100 \times 300\ \mu m^2$ focused beam of 3MeV α particles. Among the applications, micas along a drill core from the Beauvoir granite were analyzed. Bulk analyses of light elements in the drill core have previously been made. Coarse-grained micas were selected, individually irradiated and directly analyzed in polished thin sections from different elevations in the drill core. The sensitivity depends on the cross-sections of the nuclear reactions, on the particle current and on the duration of the irradiation. With a particle current irradiation of 25 nA during 1000 seconds, a 20 ppm limit of detection is reached for Be, 25 ppm for Li, 900 ppm for B and 450 ppm for F. A large variation of Be contents in the micas was found at equal drill hole elevations, and there was no strong correlation between whole-rock compositions and the mineral chemistry. The latter have been determined both by PIGE and by mineral separation and ICP analyses. On the other hand, a strong Li–F correlation was observed between the fluor-polylithionite and muscovite end-members, supporting previous analyses from equal elevation wells on sorted micas. Be–Li correlation is poorly defined, but the contents of the micas analyzed remained between the contents of bityite (Be–Li bearing mica) and lepidolites (Li-bearing micas) end-members. This suggests a solid-solution between the end-members, the extent of which is very narrow because the Be contents were not higher than 500 ppm. The detection limit is a function of the spatial resolution, because the current of the incident α (or p) particles decreases with the impact size. The results show that the analysis of small individual grains of minerals with PIGE can thus be complementary to other analytical methods such as the electronic microprobe.

The physico-chemical methods of quantitative analysis are the foundations of the interpretation of the data concerning the transportation and concentration of the chemical elements in geological contexts. Geochemical studies of granitic complexes, often in association with metallic deposits, lead to determining the mechanisms by which elements in the terrestrial crust are concentrated, which result in guidelines for mineral resources exploration. For this reason considerable studies on the geochemical and metallogenetic evolution of a granitic apex at Beauvoir-Echassières (Massif Central) have been carried out in France. The geochemistry and the petrology of this granitic massif were established on drill cores from 900 m of deep drilling,[9,15,17] Whole rock analyses were performed using wet chemistry, X-ray fluorescence and neutron

Elsevier Science S. A., Lausanne
Akadémiai Kiadó, Budapest

activation.[18] Mineral compositions were determined by electronic microprobe but, unfortunately, the light elements are not attainable by this way, and F has a poor sensitivity. In case of the light elements, the specific chemical methods which must be used require a large quantity of material after separation from the other rock-forming minerals.[15,20] The analytical results then are averages of grain sets, which erase the individual variations from which information on kinetics or equilibrium relations between phases can be attained.

However, the determination of Li, Be, B, F (O, Na Al) is possible using a sensitive, non-destructive method: analysis of prompt γ-rays emitted when a sample target is irradiated by charged particles (PIGE), e.g., protons and α. This is feasible with the aid of a Van de Graaff accelerator and a γ-spectrometer. Concerning geological materials, which are of particular interest, applications were made with the VdG 7 MV available at the Centre de Recherches Nucléaires of the CNRS in Strasbourg–Cronenbourg by various authors.[3,5,6,12] Furthermore, a probe can be made to irradiate only a small part of the sample surface when the beam of charged particles is focused with the aid of magnetic lenses. To date the impact sizes on the targets can reach down to about one μm^2.[14,19] The dimension allowed depends on the quality of the optical set, on the nature of particles, but the focusing is also limited by the need to conserve a current (incident particles flux) large enough to reach the analytical sensitivities required.

The methodologies and applications developed up to the present, have often used protons as incident particles. However, other particles can be used that have different features and feasible applications. Accordingly, a probe-turned application of the PIGE method in order to study the Be variations in individual grains of Li bearing mica in a granitic rock was performed by GALET.[11] This study used α-particles from a 3 MV VdG accelerator, focused by a quadrupolar doublet, situated in the Centre d'Etudes et de Recherches par Irradiation (CERI) at Orléans (France). The details of this application, which was used in the present study, were obtained during the perfection of a PIXE mini-probe,[2,23] which used the beam central line from switching magnet. Thus, work could only be achieved on a lateral line which did not allow the minimum beam size to be inferior to $100 \times 300\ \mu m^2$.

Among the minerals of interest, micas from the Beauvoir granite have formed the subject of a thorough study, related to previous results on the geology and geochemistry of the Echassières granitic massif (mémoire GPF, Vol. 1, 1987; document BRGM No. 124, 1988). The above 0.03 mm^2 section beam was used for analyzing individual Li-muscovites or lepidolites in the Beauvoir granite at numerous levels of the drilling. The elements Li, Be, B and F have been determined using 3 MeV monocharged α-particles. The micas-bearing targets as thin plates were submitted to the irradiation. The sample preparation is the same as that used in normal optical microscopy and for

electronic microprobe. Other materials were also analyzed for the standardization and development of methodology, and their results serve to demonstrate the capabilities of the method we have tested.

Mineralogical context

The Echassières granitic complex includes micaschists, migmatites, two out-cropping granites (one of which is the Beauvoir granite), a hidden granite and deep gneisses.[7] It is a peraluminous leucogranite suite which is one of the major types of the petrological complexes in the Hercynian belt of Europe. These complexes often contain important mineralization and thus have considerable importance in mineral exploration. The mineralization in the Echassières complex includes a W stockwerk, Sn–W and Pb–Zn ore sills, and the Sn–Li–Be–Ta deposit in the Beauvoir granite which has been partially delineated by a 900 m deep drill hole. This last rock type is an albite–topaze–lepidolite leucogranite, bulk mica compositions of which vary with the depth of sampling but remain inside the zinnwaldite–lepidolite solid solution $K_1(Li_{1.5-1}Al_{1-1.5}Fe_{0-0.5-0.25})(Si_{3-3.5}Al_{1-0.5})O_{10}(F, OH)_2$. The Li_2O and FeO contents are inversely proportional to depth, and micas at the bottom of the drill hole are larger and thicker but less numerous.[17] The Beauvoir granite contains considerable Be, with a mean whole rock content of more than 200 g/ton, which is close to being economically feasible for mining.

Accessory minerals have a great usefulness because they can characterize geochemical processes and because they are often metalbearing. In the drill core of the Beauvoir granite, these include: columbotantalite $(Fe, Mn)(Ta, Nb)_2O_6$; cassiterite SnO_2; topaz $Al_2SiO_4(F, OH)_2$; amblygonite $LiAl(PO_4)(F, OH)$; apatite $Ca_5(PO_4)_3(F, Cl, OH)$. Other accessory minerals are very rare and confined to the lower part of the drill core: fluorite CaF_2, herderite $CaBe(PO_4)(F, OH)$, beryl $Be_3Al_2(Si_6O_{18})$[1] and tourmaline $Na(Li, Al, Mg, Fe^{2+})_3Al_6(BO_3)_3(Si_6O_{18})(OH)_4$. The Be-bearing minerals are much too scarce to lead to a concentration over 200 ppm in the whole rock. Possible explanations for this high bulk Be-content are the lepidolites (Li mica), which are abundant, exhibit significant concentrations of Be, or that unidentified Be-bearing phases are present. In addition, more accurate and precise Li-contents of individual grains of micas are needed than can be calculated by difference.[10]

The thin plates bearing micas, selected such that the grain size was sufficient for the 0.03 mm^2 beam impact, are related to the following elevations of the drill hole (in meters from the top):

97.50;
108.55; 109.80; 120.05; 135.25; 189.20; 194.55; 196.20; 196.80; 197.90;
203.20; 209.20; 236.50; 259.80; 260.20; 271.45; 278.90;

367.00; 379.40;
532.90; 579.25; 599.90;

Some other minerals and light element-bearing phases not observed in the Beauvoir granite, but commonly related to granitic rocks, were also analyzed. Their formulas are: spodumene $LiAlSi_2O_6$, petalite $LiAlSi_4O_{10}$, elbaite (tourmaline) $Na(Li, Al)_3Al_6(BO_3)_3(Si_6O_{18})(OH, F)_4$, rhodizite $Na(Cs, K)Al_4(Li_4Be_3B_{10}O_{27})$, hambergite $Be_2(BO_3)(OH, F)$, synthetic Li-glass $6SiO_2$–$2.2Al_2O_3$–$1.2MgO$–$1.2Li_2O$–K_2O and obsidian $12SiO_2$–$1.6Al_2O_3$–$0.4K_2O$–$0.3Na_2O$–$0.7NaF$–$0.25Li_2O$–$0.25H_2O$.

Experimental

The Van de Graaff accelerator in the "Centre d'Etudes et de Recherches par Irradiation" (CNRS, Orléans) is a single stage machine with a 3 MV nominal voltage and a RF type ion source. After the analysis magnet and the switching magnet, a quadrupole doublet focuses the beam on the sample. The energy resolution of the charged particles is 1/1000. The measurements were made on a lateral line which permits an elliptical beam impact of a minimum size of 100×300 μm^2 to be obtained on the target sample. Care was taken to avoid abrasion of the surfaces, to limit the γ-emission rate (and consequently the dead time in the spectrometer) and to let the electrical charges flow out. Thus, in our application, the currents used were fixed around 50 nA. The analyses were performed with the aid of 3 MeV monocharged α particles because the depth of penetration is inferior to 30 μm, which permits the analysis of minerals in polished thin sections.

The irradiation device (Fig. 1) has been built such that samples can be analyzed from polished thin sections (45×30 mm^2). These 30 μm thick samples stop the 3 MeV α-particles without exciting the glass support (11 μm range for a silicate of mean density 2.7). Some rock samples and isolated minerals were included in epoxy resin cylinders (25 mm diameter and 5 mm thick), the polished surfaces of which were also submitted to particle irradiation. The surfaces of the samples are metallized with a conductive 10 nm thick layer of gold. This is essential during irradiations as long as 1000 seconds to avoid the electrical discharges which would alter the spectra. The energy loss of the 3 MeV incident α-particles through the gold deposit thickness is only 5.6 keV. An optical system allows the impact of the beam on the target to be localized with precision, and a movable X–Y mechanical system allows the chosen mineral to be positioned.

The γ-detector, a high-purity Ge of 14% efficiency, is located under the irradiation device, 45 mm from the target irradiated. It is coupled to a multichannel analyzer with a 450 MHz converter, the γ-spectra being afterwards analyzed with a computer. The

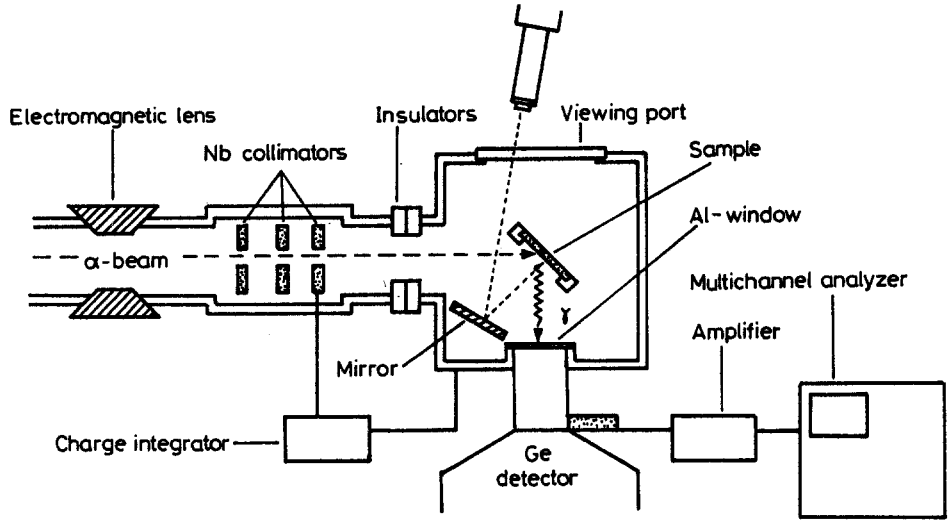

Fig. 1. Irradiation device

nuclear reactions considered in the study were mainly (α, α′) and (α, n). The Be contents were measured according to the nuclear reaction $^{9}Be(\alpha, n)^{12}C$ by the γ-transition of the excited nuclei ^{12}C at 4439 keV with simple and double escapes at 3417 and 3928 keV (in this energy field, the efficiency and resolution of the detector is weak, therefore, the impulses received in the total absorption peak and in the escape peaks were summed). For the other light elements, the following reactions were considered: $^{7}Li(\alpha, \alpha')^{7}Li$, $^{10}B(\alpha, \alpha')^{10}B$ and $^{19}F(\alpha, \alpha')^{19}F$ γ-transitions, at 478 keV, 717 keV and 197 keV respectively. Nuclear interferences can exist as for B(^{10}B), from Li: $^{7}Li(\alpha, \gamma)^{10}B$, and for Be(^{12}C) from B: $^{10}B(\alpha, d)^{12}C$.

The calculation of contents are made by relating peak areas to those of standards, similar compounds with an oxygen matrix and densities near 3. The standards used were gemstones beryl and topaz for, respectively, Be and F, amblygonite for Li, borosilicate glass for B. Each γ-peak area is divided by the number of electrical charges received by the target during its irradiation. Considering the short ranges of 3 MeV α-particles in the minerals we tested, the targets are sufficiently thick. We then made γ-yield corrections using the average stopping power of each mineral calculated according to the method of ISHII et al.[13] The averaged energies considered in this method are given by the formula

$$E_m = [\int E\sigma(E)\,dE]/[\int \sigma(E)\,dE]$$

and are calculated from the excitation functions given in Fig. 2,[6] limiting the α-energy to the 3 MeV incident value. We obtain: $E_m = 2.43$ MeV for F(α, α′), $E_m = 2.57$ MeV

Table 1
Analytical results of the Li, Be, B and F determination in minerals under 3 MeV α irradiation

SESS.	SAMPLE TARGET	DENS.	RANGE (μm)	IMP.	CUR. (nA)	FLUOR N/Q (I/nA) (197keV)	FLUOR 1 s% (N/Q) (Em=2.43MeV)	FLUOR STO.POW. (keV/μm) (Em=2.43MeV)	FLUOR F content (w%)	LITHIUM N/Q (I/nA) (478keV)	LITHIUM 1 s% (N/Q) (Em=2.57MeV)	LITHIUM STO.POW. (keV/μm) (Em=2.57MeV)	LITHIUM Li content (w%)	BORON N/Q (I/nA) (717keV)	BORON 1 s% (N/Q) (Em=2.98MeV)	BORON STO.POW. (keV/μm) (Em=2.98MeV)	BORON B content (w%)	BERYLLIUM N/Q (I/nA) (4439keV)	BERYLLIUM 1 s% (N/Q) (Em=2.18MeV)	BERYLLIUM STO.POW. (keV/μm) (Em=2.18MeV)	BERYLLIUM Be content (w%)
1	gem beryl I -1	2.70	9.2	1	37					0.2359	8.3	278.5	ppm 624					0.66668	3.0	304.0	3.996
	rhodizite -1	3.34	7.2	2	37					0.1726	9.5	358.5	588	0.04701	11.1	329.5	6.40	0.74995	5.1	391.4	5.78
	hambergite -1	2.36	9.3	2	37			282.3								250.3		1.79135	2.2	299.9	10.59
	B-silicate glass -1	2.23	11.0	6	35									0.04397	8.9	213.3	3.91				
	topaz (Th. Range) -1	3.50	7.5	4	34	1.4677	1.2	360.2	20.60												
2	gem beryl I -1	2.70	9.2	4	82					0.3479	6.4	278.5	ppm 1113					0.55055	4.3	304.0	3.996
	gem beryl II -1	2.70	9.2	4	81					0.3655	5.2	278.5	1234					0.55033	4.1	304.0	3.996
	rubellite L -1	3.05	8.2	2	76			326.3		1.7014	1.6	316.6	6189	0.01782	12.9	291.2	1.90				
	amblygonite -1	3.10	8.2	3	52	0.5187	6.5	325.9	6.27	12.8104	4.7	315.9	(%) 4.65								
3	gem beryl I -1	2.70	9.2	4	42					2.2812	0.6	278.5	ppm 5402					0.91916	1.8	304.0	3.996
	Li-glass (syn) -1	2.30	10.7	4	45					7.4452	4.6	238.5	(%) 1.51								
	spodumen -1	3.16	7.9	3	66					14.5219	0.8	283.5	3.50								
	petalite -1	2.42	10.3	3	46			259.6		9.1767	1.4	248.5	1.94								
	amblygonite -1	3.10	8.2	4	49	0.9677	3.0	325.9	6.27	17.3097	3.3	315.9	4.65								
	B-silicate glass -1	2.23	11.0	1	27									0.05765	9.6	213.3	3.91				
	Echas.203.20 -2_1	2.95	8.6	3	60	0.2895	16.2	305.1	1.72	5.0915	10.3	295.9	1.28					0.00142	33.1	323.4	ppm 56
	Echas.209.20 -1-1	2.95	8.6	2	51	0.7071	5.5	305.1	4.20	10.7719	4.3	295.9	2.71					0.00103	24.0	323.4	28
	-2-1	2.95	8.6	2	53	0.4148	4.4	305.1	2.47	6.5941	1.4	295.9	1.66					0.00103	24.0	323.4	35
	Echas.135.25 -1-1	2.95	8.6	1	42	0.6059	3.7	305.1	3.60	9.1823	0.4	295.9	2.31					0.01144	10.1	323.4	512
	-2-1	2.95	8.6	1	44	0.2118	5.4	305.1	1.26	1.9668	0.8	295.9	0.49					0.00427	16.2	323.4	194
	Echas.189.20 -1	2.95	8.6	2	43	0.7541	4.6	305.1	4.48	11.1438	6.1	295.9	2.80					0.00166	18.7	323.4	56
	Echas.236.50 -1	2.95	8.6	3	41	0.6774	2.8	305.1	4.03	9.8721	4.3	295.9	2.48					0.00178	15.9	323.4	64

	B-silicate glass -1	2.23	11.0	3	47																									
	gem beryll II -1	2.70	9.2	2	42																									
	Echas.271.45 -1	2.95	8.6	3	58	0.5483	10.2	305.1	4.35	2.1263	0.8	278.5	ppm 4447	0.04142	4.7	213.3	3.91	0.83888	1.1	304.0	(%) 3.996									
	Echas.259.80 -1	2.95	8.6	2	64	0.4459	16.9	305.1	3.53	7.2892	9.3	295.9	(%) 1.87					0.00134	15.5	323.4	ppm 51									
	Echas.278.9 -1-1	2.95	8.6	1	63	0.2706	4.3	305.1	2.15	4.8203	0.4	295.9	1.07					0.00155	13.6	323.4	63									
	-2-1	2.95	8.6	1	54	0.4236	3.6	305.1	3.36	7.0579	0.3	295.9	1.57					0.00260	15.7	323.4	122									
	Echas.194.55 -1	2.95	8.6	3	46	0.6942	4.7	305.1	5.50	10.7361	1.4	295.9	2.39					0.00175	20.9	323.4	74									
	Echas.120.05 -2	2.95	8.6	1	38	0.4801	4.2	305.1	3.81	8.7274	0.4	295.9	1.94					0.00179	13.1	323.4	88									
4																		0.00197	23.5	323.4	82									
	Echas.367 -1	2.95	8.6	2	37	0.7249	3.3	305.1	5.75	10.6733	1.8	295.9	2.37					0.00223	15.2	323.4	91									
	Echas. 97.50 -1	2.95	8.6	2	45	0.3590	5.0	305.1	2.85	6.5190	1.3	295.9	1.45					0.00160	22.2	323.4	62									
	-3	2.95	8.6	2	45	0.5869	2.3	305.1	4.73	9.0808	0.1	295.9	2.01					0.00211	17.5	323.4	88									
	Echas. 379.40	2.95	8.6	1	66	0.6942	2.4	305.1	5.42	9.8621	0.3	295.9	2.19					0.00123	28.9	323.4	42									
	Echas. 532.90 -2	2.95	8.6	1	53	0.8115	2.6	305.1	6.43	13.4476	0.2	295.9	2.99					0.00134	29.8	323.4	40									
	Echas. 579.25 -1	2.95	8.6	1	26	0.5414	4.3	305.1	4.29	7.2434	0.5	295.9	1.61					0.00461	20.0	323.4	218									
	-2	2.95	8.6	1	12	0.4684	6.9	305.1	3.72	5.7384	0.8	295.9	1.28					0.00000		323.4	0									
	Echas. 599.90	2.95	8.6	1	59	0.5880	2.7	305.1	4.66	7.9054	0.3	295.9	1.76					0.00245	19.3	323.4	108									
	topaz -1	3.50	7.5	2	66	2.0725	0.6	360.2	20.06																					
	B-silicate glass -1	2.23	11.0	2	66									0.05771	4.6	213.3	3.91													
	hambergite -1	2.36	9.3	1	29	0.0444	38.4	282.3	ppm 3372					0.03735	35.0	250.3	2.97	1.82849	0.9	299.9	(%) 8.83									
	obsidian -1	2.45	10.2	3	52	0.1823	3.5	258.0	(%) 1.13	1.5942	0.4	250.2	ppm 3015	0.00715	17.6	229.9	ppm 2192													
5	rhodizite -1	3.34	7.2	3	73	0.0387	18.1	369.6	ppm 3843	0.1286	5.6	358.5	348	0.14097	4.2	329.5	(%) 14.72	1.07717	4.6	391.4	6.82									
	gem beryl I -1	2.70	9.2	3	98					2.0585	0.6	278.5						0.83525	1.2	304.0	3.996									
	Echas. 209.20	2.95	8.6	1	154	0.4879	1.7	305.1	(%) 4.00	9.0191	0.1	295.9	(%) 2.02					0.00085	19.1	323.4	ppm 24									
	Echas. 97.50 -1-1	2.95	8.6	1	45	0.3031	3.5	305.1	2.48	3.9512	0.4	295.9	0.88					0.00066	44.7	323.4	25									
	-2-1	2.95	8.6	1	23	0.7070	3.8	305.1	5.80	9.0132	0.4	295.9	2.02					0.00091	57.9	323.4	27									
	Echas. 120.05 -2	2.95	8.6	2	25	0.4215	3.1	305.1	3.46	6.0724	0.5	295.9	1.36					0.00690	12.5	323.4	339									

SESS.	SAMPLE TARGET	DENS.	RANGE (µm)	IMP.	CUR. (nA)	FLUOR N/Q (i/nA) (197keV)	1 s% (N/Q) (Em=2.43MeV)	STO.POW. (keV/µm)	F content (w%)	LITHIUM N/Q (i/nA) (478keV)	1 s% (N/Q) (Em=2.57MeV)	STO.POW. (keV/µm)	Li content (w%)	BORON N/Q (i/nA) (717keV)	1 s% (N/Q) (Em=2.98MeV)	STO.POW. (keV/µm)	B content (w%)	BERYLLIUM N/Q (i/nA) (4439keV)	1 s% (N/Q) (Em=2.18MeV)	STO.POW. (keV/µm)	Be content (w%)
													ppm								(%)
	gem beryl I -1	2.70	9.2	3	123					1.7867	0.5	278.5	5086					0.75529	2.4	304.0	3.996
	gem beryl II -1	2.70	9.2	3	118					1.8690	3.7	278.5	5320					0.73794	2.4	304.0	304.0 3.996
	amblygonite -1	3.10	8.2	3	1132	0.6945	3.7	325.9	6.28	14.4015	2.5	315.9	(%) 4.65								3.996
	topaz (Th.Rge) -1	3.50	7.5	3	120	2.0050	12.4	360.2	20.60												
	topaz (Th.Rge) -2	3.50	7.5	3	118	2.1151	0.7	360.2	20.60												
	Echas. 579.25 -4	2.95	8.6	3	62	0.6193	3.1	305.1	5.25	8.2794	5.1	295.9	2.50					0.00196	24.9	323.4	ppm 112
6	Echas. 271.45	2.95	8.6	1	44	0.5705	2.2	305.1	4.83	8.7553	0.2	295.9	2.65					0.00157	19.4	323.4	89
	Echas. 367 -1	2.95	8.6	1	80	0.6469	1.5	305.1	5.48	9.8427	0.1	295.9	2.98					0.00084	22.3	323.4	48
	-2	2.95	8.6	1	72	0.7621	1.5	305.1	6.45	11.3360	0.1	295.9	3.43					0.00141	16.1	323.4	80
	topaz -1	3.50	7.5	2	108	2.0104	0.3	360.2	20.10												
	spodumen -1	3.16	7.9	4	117					13.0618	0.9	283.5	3.78								
	z. elbaite green -1	3.05	8.2	3	146	0.1197	5.8	326.3	1.08	3.6754	2.1	316.6	1.19	0.04319	5.0	291.2	4.67				
	red -1	3.05	8.2	3	126	0.0570	8.3	326.3	0.52	3.3060	1.1	316.6	1.07	0.04308	3.7	291.2	4.78				
	rubellite T -1	3.05	8.2	4	123	0.0347	13.2	326.3	0.31	5.3112	1.5	316.6	1.72	0.02628	15.0	291.2	1.73				
																					(%)
7	gem beryl II -1	2.70	9.2	5	23					3.2299	3.6	278.5						1.24188	2.0	304.0	3.996
													ppm								
	gem beryl II -6	2.70	9.2	1	35					2.9800	1.2	278.5	5312					1.18020	1.7	304.0	3.996
	topaz -1	3.50	7.5	8	54	2.5273	0.4	360.2	ERR												
	B-silicate glass -1	2.23	11.0	9	85									0.06393	2.4	213.3	3.91				
	spodumen -1	3.16	7.9	6	80					17.5442	0.1	283.5	(%) 3.18								
8									ppm				ppm								
	rhodizite -1	3.34	7.2	4	46	0.0487	28.3	369.6	ERR	0.1623	6.7	358.5	372	0.16285	5.7	329.5	15.3	1.38743	0.7	391.4	6.05
	hambergite -1	2.36	9.3	3	30	0.2144	12.2	282.3	(%) ERR					0.07733	24.6	250.3	5.55	3.74277	3.1	299.9	12.50
	z. elbaite red -1	3.05	8.2	2	43	0.0699	27.5	326.3	ERR	4.1791	0.6	316.6	(%) 0.85	0.06961	7.1	291.2	4.91				
	green -1	3.05	8.2	1	41	0.1561	16.1	326.3	ERR	4.3472	0.8	316.6	0.88	0.07696	9.1	291.2	5.48				

for Li(α, α'), $E_m = 2.98$ MeV for B(α, α') and $E_m = 2.18$ MeV for Be(α, n). The ranges and stopping powers of α-particles in each phase analyzed are given in Table 1, calculated using the data and compter codes of ZIEGLER et al.[22,23] The formula used

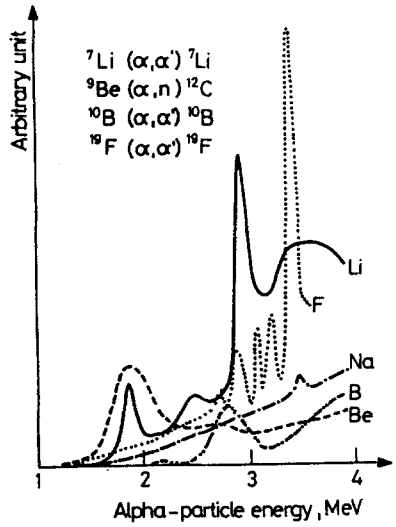

Fig. 2. Excitation functions with α-particles

for the determinations is:

$$c^m = c^{st} \cdot \{(N/Q)^m/(N/Q)^{st}\} \cdot \{(dE/dx)^m/(dE/dx)^{st}\} \quad (1)$$

where m, st – mineral and standard, respectively,
c – weight concentration,
N – net peak area (number of impulses),
Q – number of incident electrical charges,
dE/dx – stopping power of the target at the energy E_m.

The small target thickness affected by the irradiation makes the attenuation of emitted γ-rays negligible (photon energy > 200 keV), thus the intensities are measured without any correction.

Results

Measurement results of samples and standards

Table 1 shows the session numbers, the name of each of the target samples, their density, their range, the number of individual analyses performed and the mean current of irradiation, as well as for each of the four light elements, the net peak area N (impulses) divided by the number of charges Q received (N/Q ratio), the relative standard deviation s_m% of the measurement, the stopping power and the concentration calculated according to Eq. (1) and corrections needed for two nuclear interferences explained below.

The descriptions of the centimeter sized gem crystals that served as standards are given in Table 2. The hand-picked minerals, of similar origin as the Beauvoir leucogranite, are smaller than the standards but were also analyzed in polished sections. On the whole, densities lie between 2.2 and 3.5. The micas chosen in thin plates had millimeter sizes, i.e., larger than the α-beam spot. The mean density of these

Table 2
Standards used for determination of the light elements in minerals

Name	Formula	Density	Target Element	Weight content, %
Amblygonite	$LiAlPO_4$ (F, OH)	3.10	Li	4.65
Beryl	$Be_3Al_2Si_6O_{18}$	2.70	Be	3.99
Borosilicate glass	$30SiO_2$, $4B_2O_3$, $1.5Na_2O$, $0.5Al_2O_3$	2.23	B	3.91
Topaz	$Al_2SiO_4F_2$	3.50	F	20.6

lepidolites–zinnwaldites is around 3. Before depositing the gold coating, the surface of each of the three kinds of targets was polished in the same manner to keep an identical orientation relative to the beam direction and for exposure to an identical surface quality.

Thermal stability of targets

From the electrical charges received on the targets and the irradiation durations, the mean current of the monocharged α-beam was calculated for each exposure. For the isolated minerals, an average value of 55 nA was obtained for a 5 to 125 nA range, depending on the analytical session. For the polished thin sections, an average value of

40 nA was obtained for a 10 to 80 nA range. Greater currents were sometimes applied to the polished thin sections samples in order to observe the beam impact on the mineral surface and the damages provoked in the target. With a current intensity higher than 150 nA, the loosening of a mica out of the surrounding mineral assemblage was observed because of the deformation of the micaceous grain due to the disruptive discharge of this "capacitor" and resulting overheating. Knowing the beam size and the particle current, an upper limit of 3 pA/μm^2 (3 A/m^2) current density was set to avoid the destruction of the sample in our instrumental conditions. The power dissipated at the impact should then be a maximum of 9 $\mu W/\mu m^2$ (9 MW/m^2). The calculations made by BLANK and TRAXEL[4] show a negligible increase of the target temperature (1 to 10 K) when it is caused by a 1 pA/μm^2 beam of 3 MeV protons. For α-particles, which have a mass four times heavier but which are stopped in a volume four times smaller, we then observe a limit of the same order of magnitude for a temperature increase that remains acceptable for the stability of the target sample. The durations of irradiations, and then of γ-counting, were 120 to 1000 seconds for the polished thin sections but were not more than 400 seconds for the standards. The volatilization of the light elements by the α-beam has previously been the subject of specific methodological studies with the same silicate matrices but only on compressed powders.[6,12] With 3.5 MeV α-particles and 100 nA irradiation current on 1 mm^2 impact during 500 seconds, these authors observed a 8% relative decrease of F and 1% relative increase of Li (constitutive water release) in a biotite (Fe–Mg trioctahedral mica). If we consider that the evolution with time are comparable on monocrystalline samples and standards, the calculations of the light element contents may be performed directly with Eq. (1), assuming that the counting fluctuations remain within the uncertainty limits of γ-emission.

Nuclear interferences

Systematic measurements for each of the γ-spectra regions of interest (ROI) were made when one of the light elements was present and the others were absent. Thus the nuclear interferences detectable under the instrumental conditions used were quantitatively determined in relation to the peak area of the nuclide considered. The ratios $I = N/Q$ are directly compared (net sum N of the impulses in a ROI divided by the number Q of electrical charges) to make the subtraction needed in the ROI where the interference appears. Two main interferences were observed, the first from Li in the 717 keV region used for the determination of B, and the second from B in the 4439 keV region used for the determination of Be. The correction formulas fitted to the results obtained in silicates are:

for contribution of Li in the 717 keV B peak:

$$I_{717\mathrm{Li}} = 2.60 \cdot 10^{-3} \cdot I_{478}$$

$$\text{and } I_{717\mathrm{B}} = I_{717} - I_{717\mathrm{Li}}$$

for contribution of B in the 4439 keV Be peak:

$$I_{4439\mathrm{B}} = 1.57 \cdot 10^{-2} \cdot I_{717\mathrm{B}} = (1.57 \cdot 10^{-2} \cdot I_{717} - 4.08 \cdot 10^{-5} \cdot I_{478})$$

$$\text{and } I_{4439\mathrm{Be}} = I_{4439} - I_{4439\mathrm{B}}.$$

Reproducibility, precision, detection limits

The effective γ-yield Y_e depends on the conditions of focusing and counting geometry. These are different from one analytical session to another and, to minimize the uncertainty, it is better to compare the γ-peaks of samples and standards from the same session. For making a quantitative comparison between countings of samples and standards coming from two different sessions, an instrumental factor $r_{Y1} = Y_{e1} / Y_{e2}$ must be used to correct for the departure between the two individual Y_e values found in each ROI concerned. The experimental r_Y values were calculated using the second of the 8 sessions as reference ($r_{Y2} = 1 = Y_{e2} / Y_{e2}$), they are successively: $r_Y = 1.15$, 1, 1.72, 1.41, 1.50, 1.27, 2.28 and 1.94. It must be emphasized that every sample or standard that is irradiated must be polished and metallized again before each new analytical session.

The precision of the measurements can be estimated from statistics on countings (γ-rays and charges) and their reproducibility. It depends on the γ-emission yield Y, the number Q of electrical charges, the detection efficiency ε, the concentration c of the target element and its chemical evolution at the surface under the beam. The nature of the target also intervenes by producing various secondary emissions (electrons, protons, neutrons, γ-rays, bremsstrahlung and Compton diffusion) which elevates the background (BG). If the counting precision is bettter than the reproducibility, an acceptable interpretation can be attained assuming a combination of independant causes which enlarge the standard deviation: composition heterogeneity, inaccurate localization of beam, important differences in volatilization rates, rapid variation of particle current, electrical charge of target. The largest of the two kinds of uncertainties is given in Table 1, from which we can assume the following characteristic relative values (1σ in percent):

standards: Li: 3.7%, Be: 2.5%, B: 4.2%, F: 2.4%;

samples: Li: 2.4%, Be: uncertainty decreasing from 25% to 5% for contents increasing from 30 to 500 ppm, B: uncertainty decreasing from 15% to 5% for contents increasing from 0.5 to 15%, F: 8.4%.

The detection limits (*DL*) were calculated on $3\sqrt{BG}$ in the silicate matrices for 1000 second duration of irradiation with 3 MeV α-particles and beam of approximately 40 nA. They are 25 ppm for Li, 20 ppm for Be, 900 ppm for B and 450 ppm for F. The poor performance of F and B results from lower cross sections in comparison to Li and Be. A noticeable gain should be obtained with higher α-energy, e.g., 3.5 MeV.

If the irradiations had been made with 2.5 MeV protons, the *DL* of F would be 10 to 100 times lower, but 100 to 1000 times higher for Li.[6] However, in such a case, the proton range would be too great for the analysis of minerals as polished thin sections.

The detection limit for B could become lower by considering the γ-transition at 169 keV from ^{13}C according to the reaction $^{10}B(\alpha, p)^{13}C$.

The detection limit for Be would be enhanced by using a solid detector of larger efficient volume.

Geochemical application

Beryllium and lithium

Analysis of individual minerals in the Beauvoir granite has been needed because Be seems to be related to the mica phase analyzed from mineral separates. This possible correlation has to be verified and characterized at the level of the area around each mica. Choosing millimetric size grains has been forced by instrumental constraints. The hope of localizing minute Be minerals inside or outside the micas thus remains improbable because of the size of the impact beam. On the other hand, the sensitivity of the analytical method must be preserved to reach the trace level required for Be. Thus a compromise has to be considered between the ability to attain a micrometric size impact beam with a small particle current, and the need to keep a current intense enough to allow trace levels to be determined in a reasonable time.

However, with the beam used here, it is possible to estimate the presence of Be minerals included in a mica if the γ-counting rate is much higher than that of the majority of other micas. Moreover, the comparison of the Be content of individual micas to the average value from separates at the same elevation of the drill hole as well as to the bulk rock Be content, should allow this possible presence to be confirmed. In Fig. 3, Be contents of the micas are reported as a function of the drilling depth. The measurements of this study do not exactly mimic the geochemical log observed in the bulk rock nor that of the results obtained on separated micas. There is an apparent large variation of concentrations at the same elevation of the drill hole and in the same polished thin section. The use of the PIGE probe has allowed this important fact to be established. The dispersion in the deep levels (500 m) is analogous to that in higher levels (40 m) which are globally richer, but the highest individual Be-contents observed (200 to 500 ppm) are not high enough above the bulk content of the top rock (250 ppm)

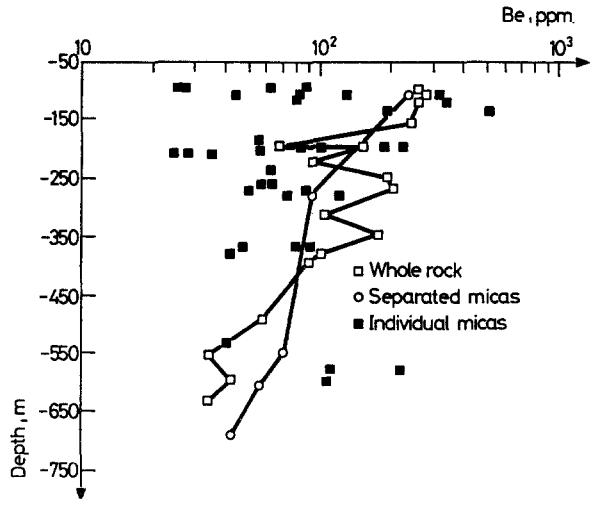

Fig. 3. Variations of the Be contents in rock, separated micas and individual micas through the Beauvoir borehole

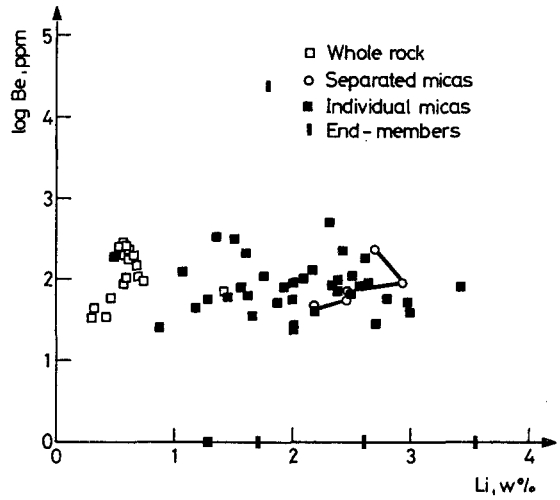

Fig. 4. Be–Li correlation in micas of the Beauvoir granite and in whole rock

to consider the existence of a Be-rich phase associated with the micas concerned. The correlation coefficient of the probe measurements is only 0.17, which does not indicate even a rough trend in comparison to the evolution of the Be content of the bulk granite (correlation coefficient of 0.82).

The Li-content of the mica is an estimation of the lepidolitization rate, thus a Be–Li correlation should be able to show the possible existence in the Beauvoir granite of a Be–Li-bearing end-member, e.g., bitiyte $Ca(Al_2Li)(Si_2AlBe)O_{10}(OH)_2$, substituted in lepidolites. Figure 4 clearly shows that lepidolites are not Be enriched relative to the rock, whatever the Li-content of the mica. All the points remain situated between the bitiyte and lepidolite end-members. The assumption of solid solution between these two end-members may not be discarded, but their substitution rate should remain very weak to respect the very low Be-contents observed (< 500 ppm). Only the determination of the Ca contents at the trace levels will allow this substitution to be confirmed. No trend is evident in Fig. 4 and the correlation coefficients calculated are low: 0.24 for individual micas and 0.39 for bulk rock. These two observations suggest that the irradiated Li-micas are not the only Be-bearing minerals, or, since only coarse-grained micas were analyzed, the fine-grained ones not analyzed have higher Be-content. This last possibility may be confirmed by comparison of the variations of Be/Li ratios with depth in micas and whole rock (Fig. 5). If the Li content of whole rock comes mainly from micas, the Be/Li ratio of whole rock, ten times lower than that of micas, shows that these micas concentrate Be. The Be/Li ratio in individual micas is similar to that of separates, 36 and 32 (ppm/%) in logarithmic averages, respectively and roughly conserves the same value all along the borehole. Then, for Be covariant with Li, fine grained micas of higher Li contents shall on the average have also higher Be contents. This possibility could be related to the mineralogical observation in the drilling that the micas are larger and less numerous at the deep elevations in comparison to the top.

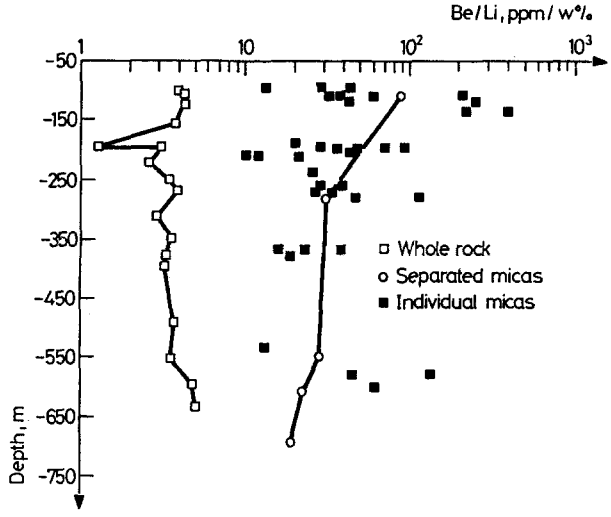

Fig. 5. Comparison of the Be/Li ratios in whole rock, separated micas and individual micas through the Beauvoir borehole

Lithium and fluorine

The PIGE method is very sensitive for Li determinatin with α-particles, which allows the concentrations at a very low trace level to be measured with a minibeam in rock-forming minerals. For F and Li, it allows the contents at the level of minor or major elements to be determined easily with great precision. The sensitivity of F could be increased by using proton irradiation, but the polished thin sections would have to be notably thicker. Concerning light elements in minerals, the direct determination of Li in individual phases has a clear usefulness in avoiding the calculations by difference needed by the electron microprobe analysis. The work of FONTEILLES[10] on this subject, dealing with the Li–Al substitutions in lepidolites in order to estimate their Li-contents from Al determination by EPMA, can be easily supported by PIGE method using proton irradiation which allows the ratio Li/Al to be directly measured.

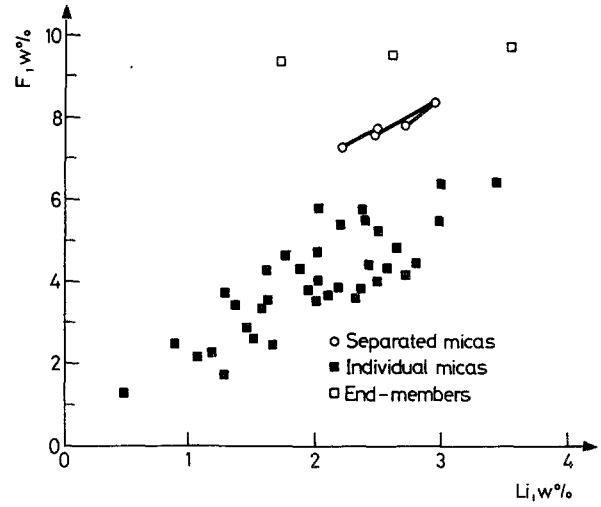

Fig. 6. F–Li correlation in micas of the Beauvoir granite

Figure 6 shows the linear correlation well marked between the end-members muscovite and fluoro-polylithionite. This grain by grain observation joins that made by MONIER et al.[15] on micas hand-picked at the same elevations of the drill hole. Such a relation easily obtained makes the slope of the corresponding regression line a feature usable to characterize fine variations in local environment of this kind of granite. In separated micas, higher F contents than in individual micas are observed, they could be explained assuming that the removal of e.g., numerous F-bearing topazes is not easy to achieve. On the other hand, it has to be noticed that PIGE method has easily determined

low Li and F contents of individual micas, which could not be performed on separated micas by conventional chemical methods.

Variations of Li contents through the Beauvoir borehole are shown in Fig. 7. They are roughly the same in whole rock and separated micas, but these cannot be compared with that of individual micas because of the too large dispersion of values. However, the

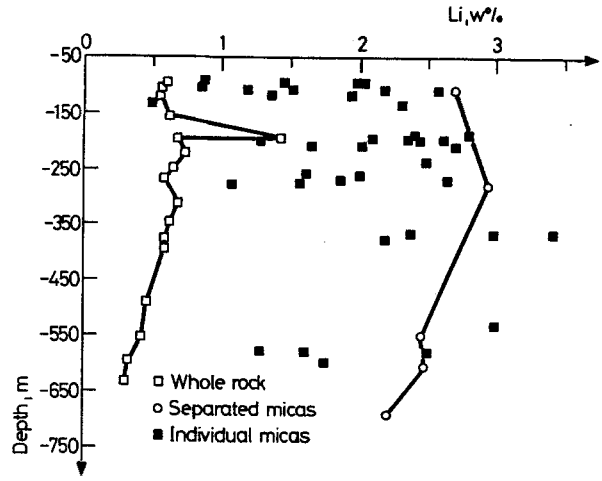

Fig. 7. Variations of Li contents in rock, separated micas and individual micas through the Beauvoir borehole

Li contents of separates are practically always higher than those of coarse-grained individual micas, thus it can be expected that the fine-grained micas contained in separates are richer in Li that the others.

Boron

This element is not enriched in the Beauvoir granite but is often present in other types of granites. The determinations were made in order to know the concentration attained with our application using standard instrumental conditions. The *DL* will be decreased using 3.5 MeV α-particles but this will not allow the trace levels expected in micas or feldspars to be determined. However, at the level of minor and major mineral components, PIGE method can easily analyze contents of B minerals in assemblages and to determine their stoichiometry, especially since they contain often Li and (or) F in variable amounts. For studies of magmatic problems about granite genesis, B can play a considerable role and thus it is of interest to determine the B content of granitic liquids. The result obtained with PIGE probe method of the "macusanite" volcanic glass from Peru,[16] agrees with the wet chemical determination previously performed.

Conclusions

The usual analysis of minerals in thin polished sections by geologists can also be performed under charged particle irradiation when the target thickness is greater than the particle range. By observing directly nuclear reactions, the method is specific to light elements, and with a focused beam thus it becomes complementary to the electron microprobe. In the geochemical investigation of a granitic context, the application of this probe method then allowed new mineralogical information to be revealed.

However, the compromise, between the ability to attain a micrometric size impact beam with a weak particle current, and the need to keep a current intense enough to allow trace levels to be attained, has to be considered for Be, B and F with α-particle beam. It was shown that it is possible to compare the Be enrichment of coexistent minerals down to a level of 100 ppm and an irradiated area of 0.03 mm^2, but much higher B and F concentrations are required with such a 40 nA beam. The very high sensitivity of Li using α-particle irradiation allow this light element to be determined at the trace level even with a much narrower spatial resolution.

Irradiation with low-energy charged particles, 2 to 4 MeV, does not only prompt nuclear reactions with the light elements, but also Coulomb interactions with heavy elements of the sample and specific X-ray emission due to the disturbance of electron layers around the nuclei. The latter effect is used by the PIXE method which performs analyses of samples for the same chemical elements as the electron microprobe. The nuclear microprobes which work on this principle, with very focused particle beams, can be applied together with the PIGE and PIXE methods if the γ- and X-rays produced can be analyzed simultaneously.

*

The authors are greatly indebted to the Director and workers of the Centre d'Etudes et de Recherches par Irradiation in Orléans who not only allowed us to use their accelerator and optical equipment but also shared knowledge on particle physics and had practical discussions about our application. We thank the Bureau de Recherches Géologiques et Minières who managed the drilling and associated research, in particular Ph. ROSSI, who supplied us with samples from Echassières in France. We also thank: V. MAGNIER-GLAVINAZ of the Ecole Normale Supérieure in Paris and F. CESBRON of Orléans University who both supplied beautiful samples from Madagascar and South America for standardization and testing. We thank very much R. L. LINNEN for interesting discussions about the geochemistry of light elements in granites and for kindly correcting the English of this paper.

References

1. G. AUBERT, Mémoire BRGM No. 46, 1969.
2. M. AZARRAH, Thèse de Doctorat d'Université, Clermont-Ferrand, France, 1993.
3. M. BASUTÇU, J.-N. BARRANDON, M. VOLFINGER, J.-L. ROBERT, Chem. Geol., 40 (1983) 353.

4. H. BLANK, K. TRAXEL, Scanning Electron Microscope, Vol. III, 1984, p. 1089.
5. B. BORDERIE, J.-N. BARRANDON, Rev. d'Archéométrie, 1 (1977) 35.
6. B. BORDERIE, Thèse d'Etat, Orsay, 1978.
7. M. CUNEY, A. AUTRAN, Mémoire GPF, Vol. 1, 1987, p. 7.
8. G. DECONNINCK, J. Radioanal. Chem., 12 (1972) 157.
9. M. FONTEILLES, Mémoire, GPF, Vol. 1, 1987, p. 149.
10. M. FONTEILLES, Documents du BRGM No. 124, Programme GPF, 1988, p. 251.
11. C. GALET, Diplôme d'Etudes Approfondies, Orléans, 1989.
12. J. HALFON et al., Compte-rendu de fin d'études DGRST,, BRGM No. 77 SGN 411 MGA, 1977.
13. K. ISHII, M. VALLADON, J.-L. DEBRUN, Nucl. Instr. Methods, 150 (1978) 213.
14. S. A. E. JOHANSSON, J. L. CAMPBELL, Micro PIXE, in: A Novel Technique for Elemental Analysis, John Wiley & Sons Ltd., 1988, p. 272.
15. G. MONIER, B. CHAROY, M. CUNEY, D. OHNENSTETTER, J.-L. ROBERT, Mém. GPF, Vol. 1, No. 2–3, 1987.
16. M. PICHAVANT et al., in: Magmatic Processes: Physicochemical Principles, B. O. MYSEN (Ed.), Geochemical Society, Special Publication, 1987, p. 359.
17. PH. ROSSI, A. AUTRAN, C. AZENCOTT, L. BURNOL, M. CUNEY, V. JOHAN, A. KOSAKEVITCH, D. OHNENSTETTER, G. MONIER, P. PIANTONE, L. RAIMBAULT, L. VIALLEFOND, Mémoire GPF, Vol. 1, 1987, p. 111.
18. PH. ROSSI, A. AUTRAN, C. AZENCOTT, K. GOVINDARAJU, G. MONIER, L. RAIMBAULT, J.-C. SAUGUES, L. VIALLEFOND, Documents du BRGM No. 124, programme GPF, 1988, p. 323.
19. J. SCHERER, K. TRAXEL, B. POVH, U. BRAUN, Max-Planck-Institut für Kernphysik, Heidelberg. Jahresbericht, 1985, p. 26.
20. R. WANG, Thèse de doctorat de l'Université Paul Sabatier, Toulouse, 1988.
21. J. F. ZIEGLER, J. P. BIERSACK, V. LITTMARCK, The Stopping and Ranges of Ions in Solids, Pergamon Press, 1985.
22. J. F. ZIEGLER, G. CUOMO, J. P. BIERSACK, The Stopping and Ranges of Ions in Matter, Computer Code TRIM88, 1988.
23. E. ZINE, D. B. ISABELLE, G. REMOND, Nucl. Instr. Methods, B49 (1990) 446.